Electronic Supplementary Material (ESI) for Physical Chemistry Chemical Physics.

Supporting information for: Switching from adduct formation to electron transfer in a light-oxygen-voltage domain containing the reactive cysteine

Kathrin Magerl, Ivan Stambolic, and Bernhard Dick*

Institute of Physical and Theoretical Chemistry, University of Regensburg, Universitaetsstrasse 31, 93053 Regensburg, Germany

E-mail: bernhard.dick@chemie.uni-regensburg.de

Phone: +49 (0)941 943 4486. Fax: +49 (0)941 943 4488

1. Mutagenesis

The gene encoding for the cDNA of *Cr*LOV1 wt was used as a template for site - directed mutagenesis. PCR was performed using *Pfu* DNA polymerase (Thermo Scientific, Waltham, MA, US) and the primers given in table S1. The sequence of the plasmids carrying the desired nucleotide substitutions was confirmed by DNA sequencing (Seqlab Sequence Laboratories, Göttingen, Germany)

Table S1: Oligonucleotide primers used for site - directed mutagenesis

Primer name	DNA base sequence (5' to 3')
CrLOV1 - F41Y - s [a]	CAGCGAGGGGTATTa[b]TGCCATGAC
CrLOV1 - F41Y - as [a]	GTCATGGCAtAATACCCCTCGCTG
CrLOV1 - C57S - s	GTGCTTGGTCACAACaGCCGCTTCCT
CrLOV1 - C57S - as	AGGAAGCGGCtGTTGTGACCAAGCAC
CrLOV1 - C57A - s	CTTGTTCACAACgcgCGCTTCCTC
CrLOV1 - C57A - as	GAGGAAGCGcgcGTTGTGACCAAG
CrLOV1 - C57G - s	gGCCGCTTCCTCCAAGGCGAGGGCACGGACCCCAA
CrLOV1 - C57G - as	CTTGGAGGAAGCGGCcGTTGTGACCAAGCACCTCATCGG

[a] s: sense primer; as: antisense primer [b] The mutated DNA bases in the specific codons are highlighted by small letters.

2. UV / Vis spectra of the different *Cr*LOV1-F41Y mutants

UV / Vis spectra of the *Cr*LOV1-F41Y mutants were recorded in the range of 300 - 600 nm using a Lambda 9a spectrometer (Perkin Elmer, Waltham, MA, US). Spectra were recorded before and after transient absorption measurements in order to control the stability of the samples.

Figure S1 shows the mutants *Cr*LOV1-F41Y, *Cr*LOV1-F41Y/C57S, *Cr*LOV1-F41Y/C57A and *Cr*LOV1-F41Y/C57G in comparison with the wild type. All mutants exhibit the typical fine structured absorption bands around 445 nm and 360 nm, showing only minor wavelength shifts compared to the wild type.

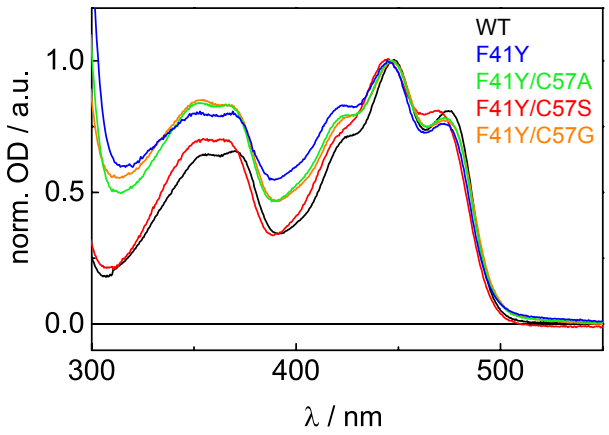

Figure S1: UV / Vis spectra of the *Cr*LOV1-F41Y mutants measured in the range of 300 - 600 nm.

Table S2: Absorption maxima of the $S_0 \rightarrow S_1$ and $S_0 \rightarrow S_2$ transitions of the *Cr*LOV1 mutants.

	$S_0 \rightarrow S_1$ (nm)	$S_0 \rightarrow S_2$ (nm)
F41Y	422 / 445 / 473	368 / 352
F41Y/C57A	424 / 446 / 473	367 / 352
F41Y/C57S	422 / 444 / 470	365 / 354
F41Y/C57G	425 / 447 / 474	368 / 354

3. Interpretation of the D_2 of *Cr*LOV1-F41Y/C57S and *Cr*LOV1-F41Y/C57A

A contribution of $FMNH^{\bullet}$ and the corresponding radical of the electron donor Tyr were assumed to be neccessary to describe the DADS associated with the slower decaying species of *Cr*LOV1-F41Y/C57S and F41Y/C57A. In the case of F41Y/C57S the linear combination of $FMNH^{\bullet}$, FMNox and $TyrO^{\bullet}$ was not sufficient to describe D_2 in figure S2A adequately. Taking into account a contribution of the FMN radical anion, $FMN^{\bullet -}$, results in the red line in figure S2A and is in good agreement with the DADS.

In contrast, D_2 of *Cr*LOV1-F41Y/C57A (figure S2B) could be best described using a linear combination of $FMNH^{\bullet}$ plus $FMN^{\bullet -}$ minus FMNox. In this case, the contribution of the FMN

radical anion is larger and the contribution of $TyrO^{\bullet}$ did not improve the spectral fitting. Thus, we can not prove unequivocably that $TyrO^{\bullet}$ is stabilized as the counter-radical of $FMNH^{\bullet}$ in *Cr*LOV1-F41Y/C57A.

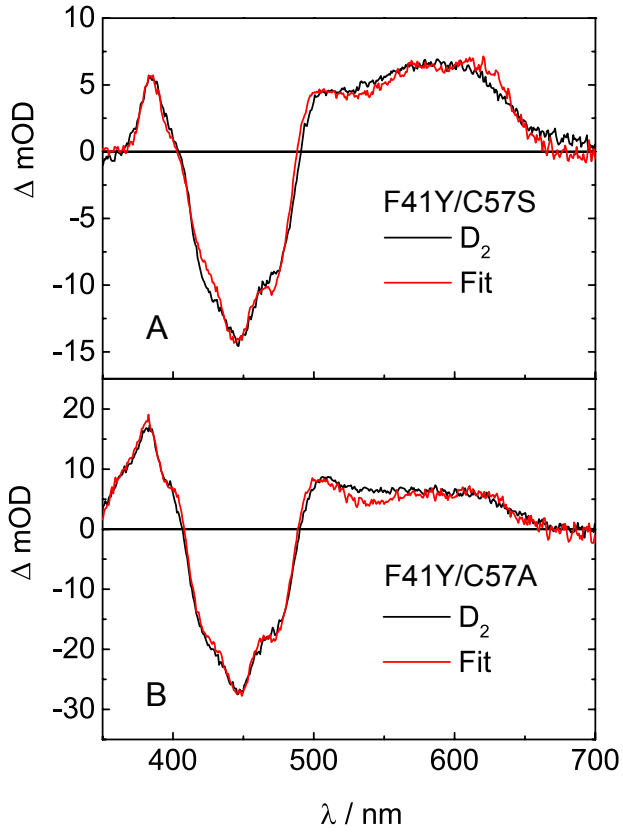

Figure S2: **A:** D_2 of *Cr*LOV1-F41Y/C57S (black line) obtained by global lifetime analysis. The spectrum could be described in good agreement by using a linear combination (fit, red line) of $FMNH^{\bullet}$, $FMN^{\bullet -}$, FMNox and $TyrO^{\bullet}$. **B:** D_2 of *Cr*LOV1-F41Y/C57A (black line) could be best described by using a linear combination (fit, red line) of $FMNH^{\bullet}$, $FMN^{\bullet -}$ and FMNox. In this case, inclusion of $TyrO^{\bullet}$ did not improve the result.

4. DADS of *Cr*LOV1-F41Y/C57G

The transient absorption measurement of *Cr*LOV1-F41Y/C57G was performed on a 100 μs streak window with laser excitation at 447 nm. Global lifetime analysis of the resulting 2D TA data matrix using two exponential functions results in the DADS shown in figure S3.

Both DADS exhibit characteristic features of the FMN triplet state indicating a biphasic triplet decay like already observed for *Cr*LOV1-C57G.[1] Further details are described in the main text of this publication. However it is noteworthy, that the ground state bleach of FMNox in D_2 is not recovering proportionally to the decrease of positive absorption signals in comparison with D_1. This is due to irreversible photo - damage of some fraction of *Cr*LOV1-F41Y/C57G during the TA measurement.

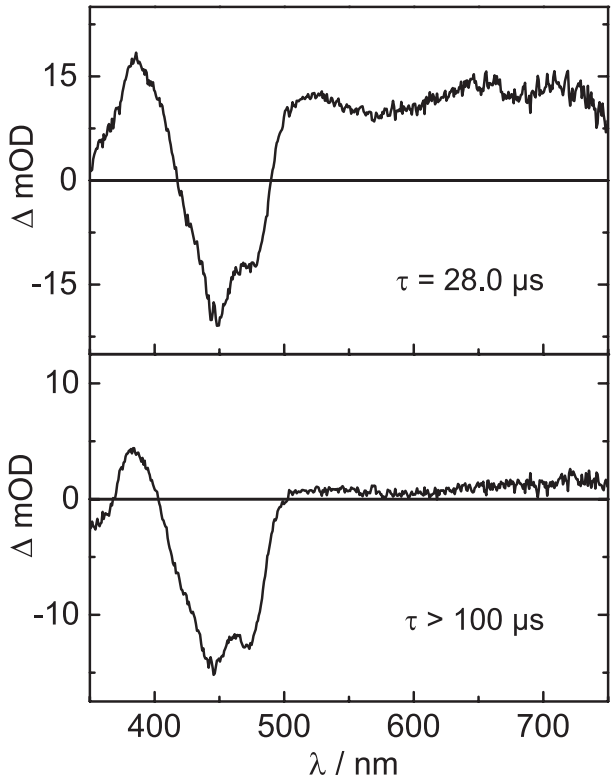

Figure S3: DADS of *Cr*LOV1-F41Y/C57G obtained by global lifetime analysis .
A: D_1 decaying with a rate constant of 28.0 μs **B:** D_2 non - decaying within 100.0 μs.

Dihedral angle distribution between F41Y and FMN

Dihedral angle distributions between Tyr41 - CE2, FMN - (C5a - C4a) and Tyr41 - CE1 of all *Cr*LOV1-F41Y mutants obtained from analyzing the 20 ns MD trajectories. The distribution curves are broad in all cases with varying maxima from 18 ° (F41Y/C57S) to 22.5 ° (F41Y).

CrLOV1-F41Y/C57A additionally has a second minor peak. The dihedral angle distribution indicate a considerable flexibility between Tyr41 and FMN possibly leading to different geometry-dependent reaction pathways.

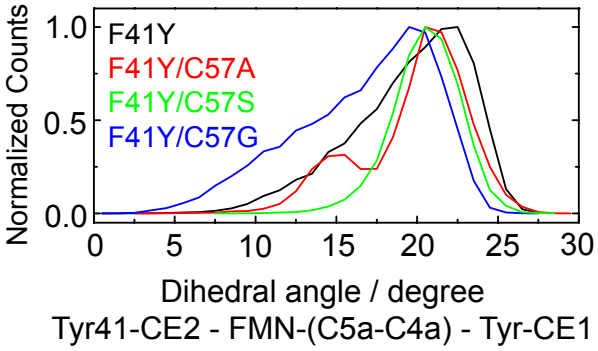

Figure S4: Dihedral angle distributions between Tyr41-CE2, FMN-(C5a-C4a) and Tyr41-CE1 of all *Cr*LOV1-F41Y mutants.

References

(1) Kutta, R. J.; Magerl, K.; Kensy, U.; Dick, B. *Photochem. Photobiol. Sci.* **2015**, *14*, 288–299.